

Langmuir-Blodgett films of Nafion-nitrogen Doped Carbon Nanotubes as New Sensing Materials for the Determination of Caffeine in Tea

Yanju Wu^{1,*}, Jianyao Kou¹, Lijie Wang¹, Long Cheng¹, Kui Lu^{2,*}

¹ Department of Material and Chemistry Engineering, Henan University of Engineering, Zhengzhou, 450007, P R China

² School of Chemical Engineering and Food Science, Zhengzhou Institute of Technology, Zhengzhou, 450044, P R China

*E-mail: yjwu2008@163.com (Dr. Yanju Wu) or lucky Luke@haue.edu.cn (Prof. Kui Lu)

Received: 17 April 2019 / Accepted: 9 September 2019 / Published: 29 October 2019

In this work, Langmuir–Blodgett (LB) technique was proposed to fabricate the homogeneous and controlled films of Nafion-nitrogen doped carbon nanotubes (Nafion-NCNTs). Microstructure and electrochemical performance of LB films of Nafion-NCNTs was characterized by atomic force microscopy (AFM) images, scanning electron microscopy (SEM) images and electrochemical experiments. Moreover, the LB film of Nafion-NCNTs was transferred to the surface of glassy carbon (GC) electrode to fabricate the electrochemical sensor to apply for determination of caffeine. Electrochemical experiments show that the LB films of Nafion-NCNTs modified GC electrode can effectively increase electrochemical response of caffeine. Under the optimum conditions, the oxidation peak current of caffeine was proportional to its concentration in the range of $8.0 \times 10^{-8} \sim 4.0 \times 10^{-6}$ mol L⁻¹, with a detection limit of 2.0×10^{-8} mol L⁻¹. And the modified GC electrode showed excellent selectivity, good stability and repeatability. It also was successfully used for determination of the content of caffeine in tea samples.

Keywords: Langmuir–Blodgett; Nafion-nitrogen doped carbon nanotubes; Caffeine; Square wave voltammetry

1. INTRODUCTION

The orderly arrangement of nanomaterial films at the molecular level for electrochemical sensor and biosensor fabrication is of extensive interest as it can not only lead to different microstructure but also change in performance characteristics [1]. Various techniques, such as robust templates [2], electron beam [3], self-assembly [4], and interface-induced ordering of nanomaterials [5], have been widely used for processing ordered nanomaterial films. Langmuir–Blodgett (LB)

method is one of the best interface-induced ordering methodologies used to manipulate materials at the molecular level [6]. LB films of different nanomaterials have been applications in piezoelectric devices [7], nonlinear optical devices [8], electrochemical sensor and biosensor [9], and so forth.

Carbon nanotubes (CNTs), due to its unique structure and electrical features, have a very attractive application prospect after its discovery in 1991 [10, 11]. Various films of CNTs-based have been explored as an electrochemical sensor and biosensor platforms [12-14]. However, the major challenge for developing of CNTs-based electrochemical sensor and biosensor is the insolubility of CNTs in all solvents. To resolve the problem, the most common route is to functionalize the surface of CNTs with organic groups or polymers [15, 16]. On the other hand, the homogeneous thin films of CNTs with precisely controlled nanostructures are an important precondition for development of high performance electrochemical sensor and biosensor. Some approaches have been reported to fabricate the homogeneous thin films of CNTs-based [16]. Meanwhile, works on the LB films of CNTs for electrochemical sensor and biosensor have been also proposed. With the aid of lithium dodecyl sulfate, Krstic and co-workers firstly fabricated matrix-diluted LB films of CNTs [17]. Gu and co-workers revealed that crown ether-modified multiwalled carbon nanotubes (MWCNTs) can also form very stable monolayers by using LB method [18]. Subsequently, different microstructure of LB films of CNTs were proposed and applied in immobilization of various biomolecules for electrochemical biosensor [19-22]. Recently, Ye and co-workers developed a novel strategy to fabricate LB films of vertically aligned multiwall carbon nanotubes-polyaniline (MWCNTs-PANI), which was used as sensing materials for determination of daidzein [23]. Despite the progress made, fabrication of CNTs with precisely controlled nanostructures is still highly desirable for the design of novel electrochemical sensors and biosensors and the improvement of the sensing performance.

Recent research confirmed that nitrogen-doped carbon nanotubes (NCNTs) exhibit better conductivity, higher rate capability and wettability than that of CNTs [24-26]. Hence, in this work, we proposed to fabricate the homogeneous and controlled thin films of Nafion-nitrogen doped carbon nanotubes (Nafion-NCNTs) based on LB film method. Atomic force microscopy (AFM) images, scanning electron microscopy (SEM) images and electrochemical experiments confirmed microstructure and excellent electrochemical performance of LB films of Nafion-NCNTs. The LB films of Nafion-NCNTs were applied as new sensing materials for the fabrication of electrochemical platform for determination of caffeine. Electrochemical experiments show that the LB films of Nafion-NCNTs can effectively increase electrochemical response of caffeine. Here, Nafion can increase the LB films character and stability of NCNTs on the surface of glassy carbon (GC) electrode due to its excellent film forming ability. And Nafion can also attract the positive charged caffeine to electrode surface effecting as accumulation.

2. EXPERIMENTAL

2.1. Materials

Nitrogen-doped multiwalled carbon nanotubes (N content: 3.00wt%; OD: 10-20 nm; L: 0.5-2 μm ; purity >95%) were supplied by Nanjing Xfnano Materials Tech. Co. Ltd. (Nanjing, China). Nafion

117 (5%, w/v in alcoholic solution) was bought from Alfa and diluted to 0.2% (w/v) with ethanol before use. All other reagents including standard sample of caffeine, KCl, $K_4[Fe(CN)_6]$, $K_3[Fe(CN)_6]$, NaH_2PO_4 and Na_2HPO_4 were purchased from Aladdin Chemistry Co., Ltd (Shanghai, China). Double distilled water (DDW) was used for all preparations. All reagents were of guaranteed reagent and were used as received.

2.2. Apparatus

Electrochemical experiments were performed at $20 \pm 0.5^\circ\text{C}$ using CHI 650A electrochemical system (CHI Instrumental, Shanghai, China) equipped with a three-electrode electrochemical cell on which was mounted a modified GC (working) electrode ($d = 3 \text{ mm}$), a platinum (counter/auxiliary) electrode, and a saturated calomel electrode (SCE) (reference) electrode. The LB films were formed and deposited on the surface of GC electrode by using a JML-04 LB trough (Shanghai, Zhongchen Co. Ltd., China). SEM (field emission scanning electron microscopic of MERLIN, Zeiss Company, Germany) and AFM (Dimension FastScan AFM, Bruker Company, Germany) were used for the morphology characterization of the prepared LB films. The pH measurements were performed with a PHS-3C precision pH meter (Leici Devices Factory of Shanghai, China).

2.3. Fabrication of the LB films of Nafion-NCNTs modified GC electrode

GCE were properly polished with alumina ($0.05 \mu\text{m}$) slurries, and rinsed with DDW and then sequentially ultrasonicated in ethanol and DDW before modification or use. A homogenous suspension of Nafion-NCNTs (0.5 mg mL^{-1}) was obtained by ultrasonication for 0.5 h. Then, the suspension of Nafion-NCNTs was spread on the subphase drop by drop. After the evaporation of ethanol solvent for 30 min, the suspension of Nafion-NCNTs was spread all over the surface of subphase and a stable floating film was obtained. The monolayer of Nafion-NCNTs was compressed with a rate of 9.71 mm min^{-1} and then transferred onto the GC electrode (vertical dipping) at a rate of 1.02 mm min^{-1} under a surface pressure of 20 mN m^{-1} . This fabricated electrode was named Nafion-NCNTs-LB/GCE. For comparison, a Nafion modified GC electrode were fabricated with the similar procedure, named Nafion-LB/GCE. The fabricated modified GC electrodes were kept in DDW when they were not in use.

2.4. Preparation of tea samples

The commercial tea was purchased from local supermarket (Zhengzhou, China). 10 g tea was weighed, and soaked adequately in 500 mL DDW (90°C). The supernatant were filtered, and an appropriate amount of filtrate was directly added to the supporting electrolyte for the determination of caffeine.

3. RESULTS AND DISCUSSION

3.1. π -A isotherms

It is reported that CNTs themselves cannot form stable LB film, but Nafion can in the presence of Na^+ [27]. Here, we presented to fabricate LB films of Nafion-NCNTs in the presence of K^+ . Nafion can increase the LB films character and stability of NCNTs due to its excellent film forming ability. **Fig.1** shows the surface pressure (π) versus trough area (A) (π -A) isotherms of Nafion-NCNTs on DDW (curve a), and NCNTs (curve b), Nafion (curve c), Nafion-NCNTs (curve d) on aqueous subphase containing $1.0 \times 10^{-2} \text{ mol L}^{-1} \text{ KCl}$. Using DDW as the subphase, Nafion-NCNTs does not show any sharp increase in the π -A isotherm, indicating the sinking of Nafion-NCNTs below the air/water interface due to the partial solubility of Nafion in water. Interestingly, the shape of isotherms changes dramatically when KCl are added to the aqueous subphases. The remarkable variation in the π -A isotherm of Nafion-NCNTs might be the presence of K^+ in the subphase. In this case, Nafion-NCNTs cannot sink, but floats at the air/water interface. The role of K^+ in the subphase is to stabilize the sulfonic groups of Nafion, which is similar to that of Na^+ in previously reports [27]. Moreover, the isotherm of Nafion-NCNTs are shifted to higher areas, compared with the π -A isotherms of NCNTs and Nafion. The result confirmed that the NCNTs have been introduced into the films of Nafion.

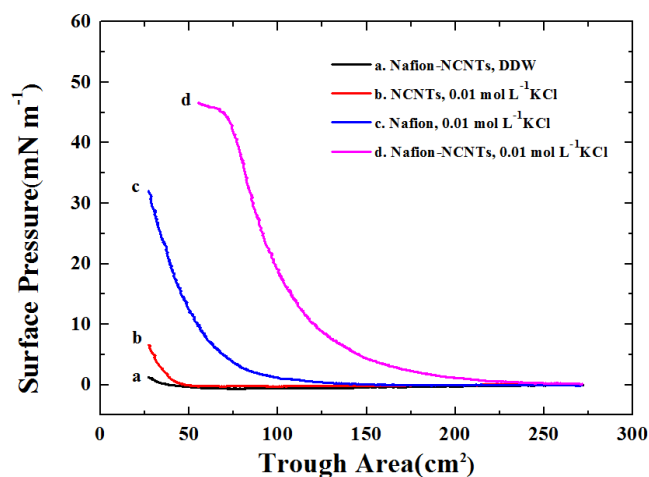


Figure 1. π ~ A isotherms of Nafion-NCNTs on DDW (curve a), and π ~ A isotherms of NCNTs (curve b), Nafion (curve c) and Nafion-NCNTs (curve d) on aqueous subphase containing $1.0 \times 10^{-2} \text{ mol L}^{-1} \text{ KCl}$.

3.2. Characterization of LB films of Nafion-NCNTs nanocomposite

Fig.2 shows a typical AFM 2D morphology images of the freshly cleaned mica covered with 1 layer of LB films of Nafion (A) and Nafion-NCNTs (B) under transfer surface pressures of 20 mN m^{-1} . It is clear that uniform and dense LB films of Nafion were observed. When the NCNTs were introduced, orderly arranged and snake-like nanotubes without aggregation were well-dispersed on the surface of GC electrode. SEM images for LB films of Nafion-NCNTs also show the same results (**Fig. 3**). Moreover, aged LB samples for the films of Nafion-NCNTs show little changes, indicating the

stability of the LB films. This result also indicated that LB films of Nafion-NCNTs modified on the surface of GC electrode have good stability.

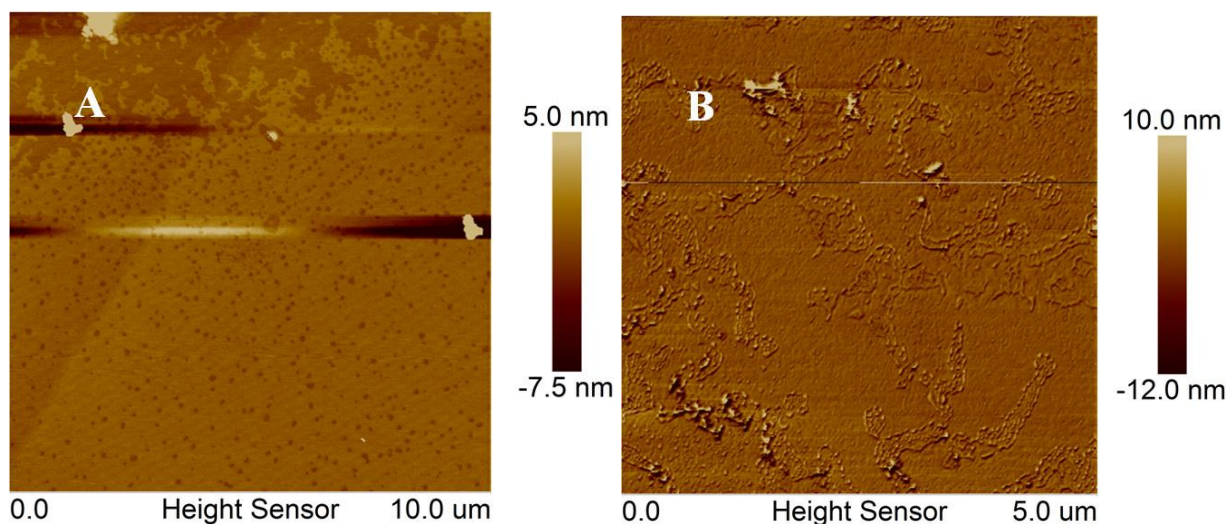


Figure 2. AFM 2D morphology images of the freshly cleaned mica covered with 1 layer of LB film of Nafion (A) and Nafion-NCNTs (B) under transfer surface pressures of 30 mN m^{-1} .

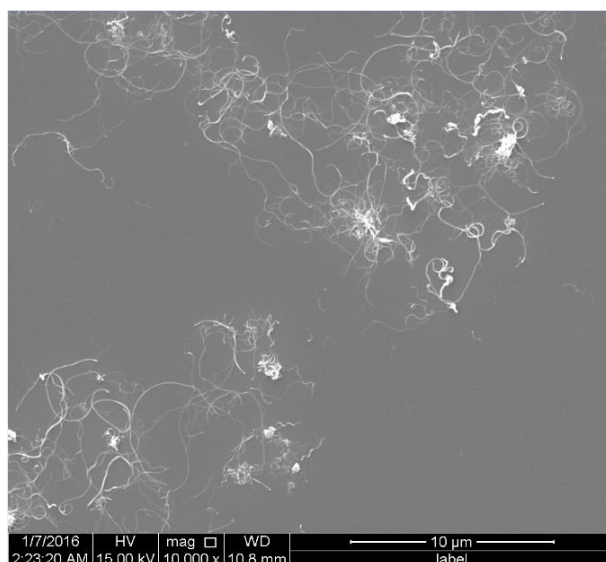


Figure 3. SEM image obtained from Nafion-NCNTs -LB/GCE.

For evaluating the characteristic of the LB film of Nafion-NCNTs, $\text{K}_3[\text{Fe}(\text{CN})_6]/\text{K}_4[\text{Fe}(\text{CN})_6]$ (1:1) was chosen and electrochemical impedance spectroscopy (EIS) was performed. At the high frequency region, a small well-defined semicircle was observed at the bare GCE (**Fig.4**), indicating low interface electron resistance (R_{ct}). When the Nafion-LB/GCE was applied, the diameter of the semicircle obviously increased suggesting that the introduction of the negatively charged LB film of Nafion hampers the electron transfer. However, the diameter of the semicircle decreased remarkably

after NCNTs was introduced into the LB films of Nafion due to the high conductivity of NCNTs. In further research, an equivalent circuit was proposed as showed in the inset of **Fig.4**. The R_{ct} was obtained to be $86\ \Omega$, $3580\ \Omega$ and $3104\ \Omega$ for the bare GCE, Nafion-LB/GCE and Nafion-NCNTs-LB/GCE by using fitting calculation, respectively. Meanwhile, a linear relationship between the number of layers and the R_{ct} was found (the inset of **Fig.4**), indicating the films are uniform, controllable and repeatable. These performances are highly helpful in fabricating an interface for the electrochemical sensors.

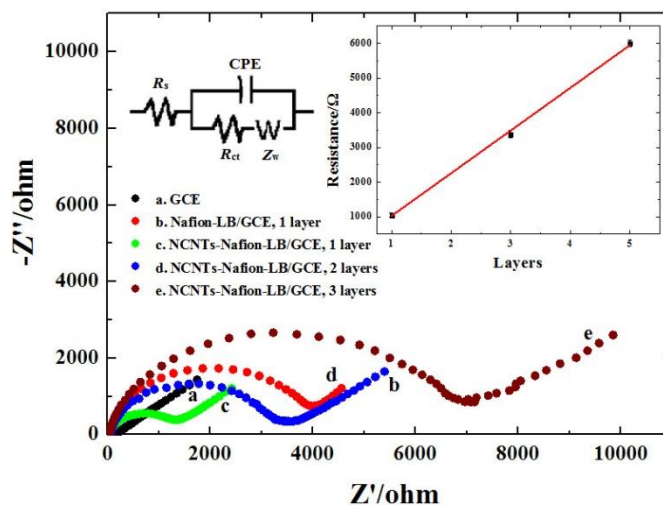


Figure 4. Nyquist plots of bare GCE (curve a), Nafion-LB/GCE (curve b) and different layer Nafion-NCNTs-LB modified GC electrode in $5 \times 10^{-3} \text{ mol L}^{-1} \text{ Fe(CN)}_6^{3-/4-} + 0.2 \text{ mol L}^{-1} \text{ KCl}$ solution (curve c: 1 layer, curve d: 3 layer, curve e: 5 layer); the frequency range is from 1 MHz to 0.01 Hz, and the perturbation signal is 5 mV; the inset is equivalent circuit and the relationship between layer number and the resistance.

3.3. Electrochemical characterization of caffeine at the Nafion-NCNTs-LB/GCE

The electrochemical behavior of caffeine on the surface of both bare and modified electrodes was investigated by cyclic voltammetry (CV). **Fig.5A** shows the cyclic voltammograms (CVs) obtained for the bare GCE (curve a), Nafion-LB/GCE (curve b) and Nafion-NCNTs-LB/GCE (curve c) in the presence of $2.0 \times 10^{-6} \text{ mol L}^{-1}$ caffeine in $0.1 \text{ mol L}^{-1} \text{ H}_2\text{SO}_4$ (pH = 0.94) at a scan rate of 0.05 V s^{-1} , respectively. Obviously, the bare GCE showed a very weak oxidation peak current response of $1.39 \mu\text{A}$ for caffeine at 1.45 V. At the Nafion-LB/GCE, caffeine yielded a higher oxidation peak current response of $5.29 \mu\text{A}$ at 1.44 V. The result confirms that the homogeneous LB films of Nafion can attract the positive charged caffeine to electrode surface as accumulation. Meanwhile, the best performance was achieved at the Nafion-NCNTs-LB/GCE, which reached the maximum current response of $12.87 \mu\text{A}$ for caffeine at 1.42 V. This can be explained in consideration of both the increased surface area of the electrode and the enhanced conductivity due to the addition of NCNTs into LB films of Nafion. Moreover, the oxidation peak current response grows with the increasing of the number of modified layers. A linear relationship between peak current response and the number of

layers was found when the number of layers is less than 3 (not show). These results indicated that the LB films of Nafion-NCNTs are precisely controllable and repeatable.

The influence of the scan rate on the electrocatalytic oxidation of caffeine at the Nafion-NCNTs-LB/GCE was investigated by CV within a range of $0.05 \sim 0.40 \text{ V s}^{-1}$ (see **Fig.5B**). The oxidation peak currents grow with the increasing of scan rate, and the logarithm of oxidation peak currents versus scan rates exhibited a linear relationship with a slope of 0.716 (see the inset of **Fig.5B**), demonstrating that the electrode reaction process of caffeine was driven by mixture of diffusion and adsorption controlled process [28].

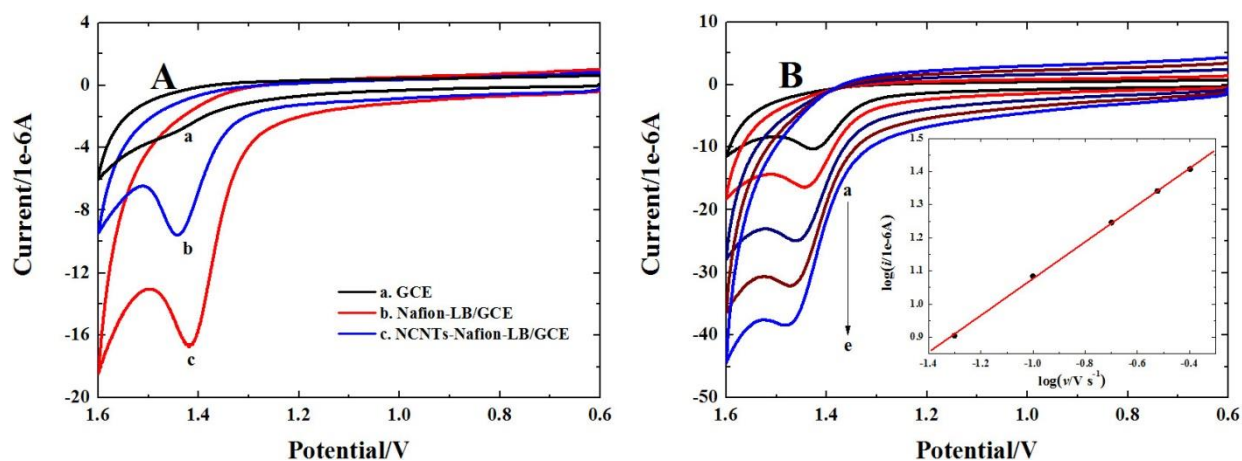


Figure 5. (A) CVs of $2.0 \times 10^{-6} \text{ mol L}^{-1}$ caffeine at bare GCE (curve a), Nafion-LB/GCE (curve b) and Nafion-NCNTs-LB/GCE (curve c) in $0.1 \text{ mol L}^{-1} \text{ H}_2\text{SO}_4$ ($\text{pH} = 0.94$), $v = 0.05 \text{ V s}^{-1}$; (B) CVs of $2.0 \times 10^{-5} \text{ mol L}^{-1}$ codeine at Nafion-NCNTs-LB/GCE at different scan rate (from a to e: $0.05, 0.10, 0.20, 0.30, 0.40 \text{ V s}^{-1}$); the insert shows the relationship of $\log i_{pa}$ and $\log v$.

3.4. Square wave voltammetry and chronoamperometry investigations

Square wave voltammetry (SWV) was used to obtain a higher oxidation peak current response. **Fig.6A** shows square wave voltammograms (SWVs) in different frequency (scan increment: 4 mV ; pulse amplitude: 25 mV). The oxidation peak currents grow with the frequency, and a good linear equation (in the range of $10\text{-}30 \text{ Hz}$) was represented as $i_p(\mu\text{A}) = 2.64 + 0.135f(\text{Hz})$ ($R = 0.998$). From the slope of this straight line according to previous reports [29], saturating absorption capacity (I^*) for caffeine at the Nafion-NCNTs-LB/GCE was obtained to be $(5.24 \pm 0.27) \times 10^{-10} \text{ mol cm}^{-2}$. The result is higher than that of bare GCE ($(3.47 \pm 0.28) \times 10^{-10} \text{ mol cm}^{-2}$) and Nafion-LB/GCE ($(7.84 \pm 0.21) \times 10^{-11} \text{ mol cm}^{-2}$). It is therefore confirmed that the LB films of Nafion-NCNTs is effective for enlargement the loading amount of caffeine due to the increase in the effective surface area.

Chronoamperometry (CA) was also performed to evaluate the catalytic rate constant (k_{cat}) for the oxidation of caffeine at the Nafion-NCNTs-LB/GCE. **Fig.6B** shows chronoamperograms of Nafion-NCNTs-LB/GCE in the absence (curve a), $5.0 \times 10^{-5} \text{ mol L}^{-1}$ (curve b), $1.0 \times 10^{-4} \text{ mol L}^{-1}$ (curve c) and $2.0 \times 10^{-4} \text{ mol L}^{-1}$ (curve d) caffeine. From the slope of the straight line for the corresponding i_{cat}/i_L versus $t^{1/2}$ plot according to previous report (see the inset of **Fig.6B**) [30, 31], the k_{cat} is calculated to be

$8.67 \times 10^2 \text{ mol L}^{-1} \text{ s}^{-1}$ for $1.0 \times 10^{-4} \text{ mol L}^{-1}$ caffeine, which is much larger than that of bare GCE ($74.8 \text{ mol L}^{-1} \text{ s}^{-1}$) and Nafion-LB/GCE ($4.67 \times 10^2 \text{ mol L}^{-1} \text{ s}^{-1}$). The result verifies Nafion-NCNTs-LB/GCE can provide a more efficient interface for the oxidation of caffeine.

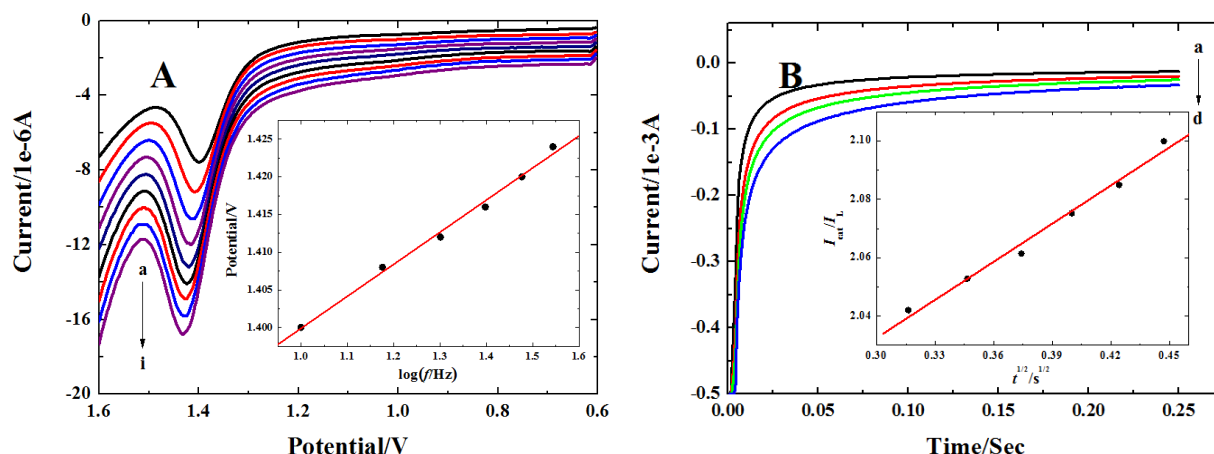


Figure 6. (A) SWASVs of $2.0 \times 10^{-6} \text{ mol L}^{-1}$ caffeine at Nafion-NCNTs-LB/GCE in different frequency (from a to i: 10Hz, 15Hz, 20Hz, 25Hz, 30Hz, 35Hz, 40Hz, 45Hz and 50Hz), scan increment of 4 mV and pulse amplitude of 35 mV; (B) Chronoamperograms of Nafion-NCNTs-LB/GCE in $0.1 \text{ mol L}^{-1} \text{ H}_2\text{SO}_4$ (pH = 0.94) solution containing (a) 0, (b) 50, (c) 100 and (d) 200 $\mu\text{mol L}^{-1}$ caffeine; the insert shows the relationship of i_{cat}/i_L versus $t^{1/2}$ for $100 \mu\text{mol L}^{-1}$ caffeine.

3.5. Electrochemical detection of caffeine at the Nafion-NCNTs-LB/GCE

The optimum conditions were chosen as: the number of layers: 3 layers; accumulation time (t_{acc}): 180 s; accumulation potential (E_{acc}): open circuit. The parameters of SWV were selected as: scan increment: 4 mV; pulse amplitude: 25 mV; frequency: 30 Hz. Under the optimum conditions, the calibration curve for the determination of caffeine was established. **Fig.7A** shows the response of different concentration of caffeine by square wave adsorptive stripping voltammetry (SWASV). A linear relationship between the electrochemical response and caffeine concentrations in the range of $8.0 \times 10^{-8} \sim 4.0 \times 10^{-6} \text{ mol L}^{-1}$ was observed as represented by the following equations: $i_{pa}(\mu\text{A}) = 0.853 + 5.788c(\mu\text{mol L}^{-1})$, ($R = 0.999$). Standard deviations (SD) for the slope and intercept of the calibration curve were 0.0027 and 0.015, respectively. Based on the signal-to-noise ratio of 3 (S/N) [32], the detection limit was obtained as $2.0 \times 10^{-8} \text{ mol L}^{-1}$.

The reproducibility and stability of the Nafion-NCNTs-LB/GCE were investigated by SWASV in $0.1 \text{ mol L}^{-1} \text{ H}_2\text{SO}_4$ containing $2.0 \times 10^{-6} \text{ mol L}^{-1}$ caffeine. The five successive tests at same Nafion-NCNTs-LB/GCE show relative standard deviation of 3.1%. For stability of the Nafion-NCNTs-LB/GCE, a same caffeine solution was detected on day one and a month later. The oxidation peak current of caffeine recorded on day one and a month later were changed about 4.7%. These experiments indicate that the Nafion-NCNTs-LB/GCE has excellent reproducibility and stability for the determination of caffeine.

The influence of theophylline on the detection of caffeine was evaluated. **Fig.7B** shows square

wave adsorptive stripping voltammograms (SWASVs) of Nafion-NCNTs-LB/GCE in 0.1 mol L⁻¹ H₂SO₄ solutions containing 2.0 × 10⁻⁶ mol L⁻¹ caffeine and different concentrations of theophylline. It is obvious that two well-defined oxidation peaks appeared at the potentials of 1.29 V and 1.42 V for theophylline and caffeine, respectively. The result not only indicates the Nafion-NCNTs-LB/GCE have excellent selective sensing for caffeine, but also can be used to simultaneous detection of caffeine and theophylline.

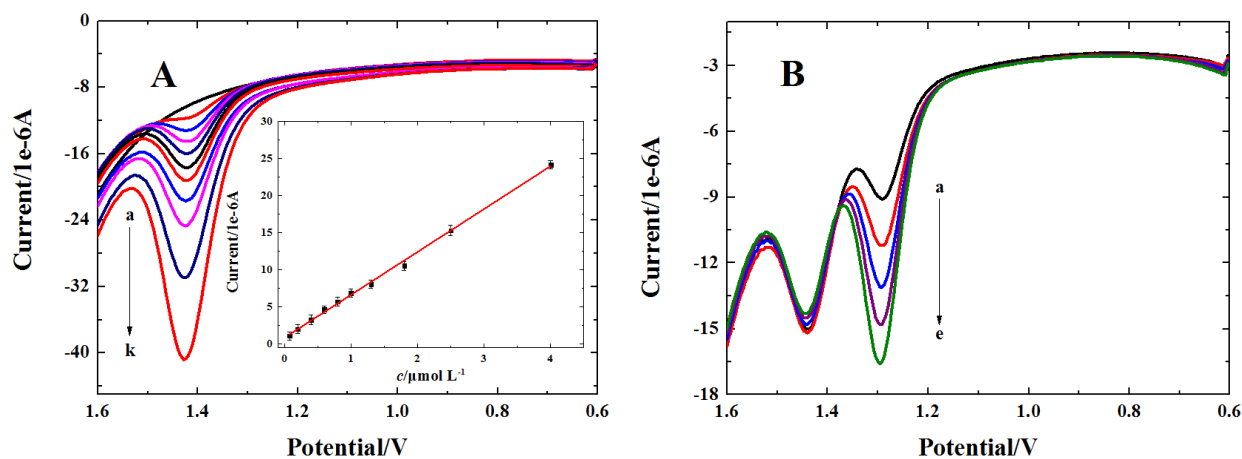


Figure 7. (A) SWASVs and their associated calibration plot (insert) for increasing concentrations of caffeine at Nafion-NCNTs-LB/GCE under optimum conditions; (B) SWASVs of Nafion-NCNTs-LB/GCE in 0.1 mol L⁻¹ H₂SO₄ solutions containing 2.0 × 10⁻⁶ mol L⁻¹ caffeine and different concentrations of theophylline

The method proposed was compared with a different CNTs-based electrochemical sensor reported for determination of caffeine (see **Table 1**). The proposed method gives a reasonably lower detection limit and wider linear range. The reason mainly depends on the performances of uniform and dense LB films of Nafion-NCNTs. The result suggests also that the LB films of Nafion-NCNTs as voltammetric sensing materials might be a very promising platform.

Table 1. Comparison of determination of caffeine by different CNTs-based electrochemical sensor reported.

Modified electrodes	Methods	Linear range	Detection limit (mol L ⁻¹)	Reference
MWCNTs-Nafion/GCE	DPASV	2.945×10 ⁻⁶ ~ 3.770×10 ⁻⁴ 3.770×10 ⁻⁴ ~ 2.356×10 ⁻³	5.13×10 ⁻⁷	[26]
DNA-SWCNTS/Nafion/GCE	SWASV	5.0×10 ⁻⁷ ~ 1.0×10 ⁻⁴	1.0×10 ⁻⁷	[33]
Nafion/GCE	DPV	9.95×10 ⁻⁷ ~ 1.06×10 ⁻⁵	7.79 × 10 ⁻⁷	[34]
MWCNTs-Nafion/GCE	DPV	6.0×10 ⁻⁷ ~ 4.0×10 ⁻⁴	2.3 × 10 ⁻⁷	[35]
SWCNTs/CCE	DPV	4.0×10 ⁻⁷ ~ 3.0×10 ⁻⁴	2.5×10 ⁻⁷	[36]
ENGR-NCNTs/GCE	SWV	6.0×10 ⁻⁸ ~ 5.0×10 ⁻⁵	2.0×10 ⁻⁸	[37]

poly(AV3B)/MWCNTs-GR/GCE	DPV	$1.0 \times 10^{-6} \sim 1.2 \times 10^{-4}$	1.0×10^{-7}	[38]
ZnO/MWCNTs/GCE	DPV	$2.0 \times 10^{-8} \sim 2.5 \times 10^{-5}$	1.0×10^{-8}	[39]
PLCY/NCNTs/GCE	DPV	$4.0 \times 10^{-7} \sim 1.4 \times 10^{-4}$	2.0×10^{-7}	[40]
PDA/AuNPs/GCE	DPV	-	7.9×10^{-7}	[41]
Nafion-NCNTs-LB/GCE	SWASV	$8.0 \times 10^{-8} \sim 4.0 \times 10^{-6}$	2.0×10^{-8}	This work

CCE: carbon-ceramic electrode;

poly(AV3B): poly(Alizarin Violet 3B);

PLCY: poly(L-Cysteine);

PDA/AuNPs: polydopamine-gold nanocomposite;

GR: Graphene;

ENGR: electrodeposited nitrogen-doped graphene;

DPV: differential pulse voltammetry;

DPASV: differential pulse adsorptive stripping voltammetry;

SWASV: square wave adsorptive stripping voltammetry;

3.6. Determination of caffeine in tea samples

To evaluate the practical application of Nafion-NCNTs-LB/GCE, it was used to determine the content of caffeine in tea samples. For evaluating the veracity, caffeine standard solution was added to calculate the recovery. The results were listed in Table 2. The values of recovery are calculated to be over the range from 95.7 to 100.3%, indicating that the newly-developed modified electrode is accurate and has promising application.

Table 2. Determination results of caffeine in some tea samples by SWASV (n=5)

Sample	Amount found	R.S.D. (%)	Standard added	Total found	Recovery (%)
Green tea	20.15 mg g ⁻¹	3.7	20.00 mg g ⁻¹	40.20 mg g ⁻¹	100.3
Black tea	28.75 mg g ⁻¹	2.8	20.00 mg g ⁻¹	47.89 mg g ⁻¹	95.7
Oolong tea	24.87 mg g ⁻¹	3.1	20.00 mg g ⁻¹	44.31 mg g ⁻¹	97.2

4. CONCLUSIONS

In the current report, we described to fabricate the homogeneous and controlled thin films of Nafion-NCNTs based on LB film method. The LB films of Nafion-NCNTs were successfully applied as new sensing materials for the fabrication of electrochemical platform for determination of caffeine. The data reported here showed that the proposed method gives a reasonably lower detection limit and

wider linear range. And the newly-developed modified electrode has excellent selectivity, good stability and repeatability.

ACKNOWLEDGMENTS

The authors would like to thank the financial sponsored by the National Science Foundation of China (No. 21572046) and the key scientific research projects in Universities of Henan Province (No. 16A150029).

References

1. J. Rivnay, L. H. Jimison, J. E. Northrup, M. F. Toney, R. Noriega, S. Lu, T. J. Marks, A. Facchetti, A. Salleo, *Nat. Mater.*, 8 (2009) 952.
2. J. H. Park, Y. L. Joo, *Appl. Surf. Sci.*, 416 (2017) 742.
3. S. Y. Xu, M. L. Tian, J. G. Wang, H. Xu, J. M. Redwing, M. H. Chan, *Small*, 1 (2005) 1221.
4. E. Royston, A. Ghosh, P. Kofinas, M. T. Harris, J. N. Culver, *Langmuir*, 24 (2008) 906.
5. S. Xie, S. Bao, J. Ouyang, X. Zhou, Q. Kuang, Z. Xie, L. Zheng, *Chem-Eur. J.*, 20 (2014) 5244.
6. S. Sangiao, S. Martin, A. Gonzalez-Orive, C. Magen, P. J. Low, J. M. Teresa, P. Cea, *Small*, 13 (2017).
7. I. Azad, M. K. Ram, D. Y. Goswami, E. Stefanakos, *Langmuir*, 32 (2016) 8307.
8. A. Colombelli, M. G. Manera, V. Borovkov, G. Giancane, L. Valli, R. Rella, *Sensor. Actuat. B-Chem.*, 246 (2017) 1039.
9. L. Caseli, J. R. Siqueira, *Langmuir*, 28 (2012) 5398.
10. S. Frank, P. Poncharal, Z. L. Wang, W. A. deHeer, *Science*, 280 (1998) 1744.
11. P. Avouris, *Accounts Chem. Res.*, 35 (2002) 1026.
12. M. M. Barsan, M. E. Ghica, C. M. Brett, *Anal. Chim. Acta*, 881 (2015) 1.
13. Q. Zhao, Z. H. Gan, Q. K. Zhuang, *Electroanal.*, 14 (2002) 1609.
14. Q. Zhao, M. B. Nardelli, W. Lu, J. Bernholc, *Nano Lett.*, 5 (2005) 847.
15. C. Gao, Z. Guo, J. H. Liu, X. J. Huang, *Nanoscale*, 4 (2012) 1948.
16. A. J. S. Ahammad, J. J. Lee, M. A. Rahman, *Sensors*, 9 (2009) 2289.
17. V. Krstic, G. S. Duesberg, J. Muster, M. Burghard, S. Roth, *Chem. Mater.*, 10 (1998) 2338.
18. L. Feng, H. J. Li, F. Y. Li, Z. J. Shi, Z. N. Gu, *Carbon*, 41 (2003) 2385.
19. Q. Sun, N. A. Zorin, D. Chen, M. Chen, T. X. Liu, J. Miyake, D. J. Qian, *Langmuir*, 26 (2010) 10259.
20. A. R. Liu, T. Wakayama, C. Nakamura, J. Miyake, N. A. Zorin, D. J. Qian, *Electrochim. Acta*, 52 (2007) 3222.
21. A. R. Liu, D. J. Qian, T. Wakayama, C. Nakamura, J. Miyake, *Colloid Surfaces A.*, 284 (2006) 485.
22. Q. Sun, J. Liu, M. Chen, J. Miyake, D. J. Qian, *J. Nanosci. Nanotechnol.*, 14 (2014) 5468.
23. L. Wang, Y. Li, Q. Wang, L. Zou, B. Ye, *Sensors Actuat. B-Chem.*, 228 (2016) 214.
24. M. Vikkisk, I. Kruusenberg, U. Joost, E. Shulga, K. Tammeveski, *Electrochim. Acta*, 87 (2013) 709.
25. N. G. Tsierkezos, S. H. Othman, U. Ritter, *Ionics*, 19 (2013) 1897.
26. J. Zhang, L. P. Wang, W. Guo, X. D. Peng, M. Li, Z. B. Yuan, *Int. J. Electrochem. Sc.*, 6 (2011) 997.
27. P. Bertonecello, M. K. Ram, A. Notargiacomo, P. Ugo, C. Nicolini, *Phys. Chem. Chem. Phys.*, 4 (2002) 4036.
28. Y. F. Li, L. N. Zou, G. Song, K. J. Li, B. X. Ye, *J. Electroanal. Chem.*, 709 (2013) 1.
29. M. Lovric, S. Komorskylovic, R. W. Murray, *Electrochim. Acta*, 33 (1988) 739.
30. F. Wang, Y. J. Wu, K. Lu, L. Gao, B. X. Ye, *Electrochim. Acta*, 141 (2014) 82.
31. M. H. Pournaghi-Azar, R. Sabzi, *J. Electroanal. Chem.*, 543 (2003) 115.
32. J. N. Miller, J. C. Miller, *Statistics and Chemometrics for Analytical Chemistry, fourth ed*, Pearson Education Limited: London, (2000).

33. Y. W. Wang, X. H. Wei, F. Wang, M. Li, *Anal. Methods*, 6 (2014) 7525.
34. B. Brunetti, E. Desimoni, P. Casati, *Electroanal.*, 19 (2007) 385.
35. S. Yang, R. Yang, G. Li, L. Qu, J. Li, L. Yu, *J. Electroanal. Chem.*, 639 (2010) 77.
36. B. Habibi, M. Abazari, M. H. Pournaghi-Azar, *Colloid. Surface. B.*, 114 (2014) 89.
37. L. Jiang, Y. Ding, F. Jiang, L. Li, F. Mo, *Anal. Chim. Acta*, 833 (2014) 22.
38. Y. Wang, T. Wu, C. Bi, *Microchim. Acta.*, 183 (2016) 731.
39. T. Muzvidziwa, M. Moyo, J. O. Okonkwo, M. Shumba, T. Nharingo, U. Guyo, *Int. J. Environ. An. Ch.*, 97 (2017) 623.
40. Y. Wang, Y. Ding, L. Li, P. Hu, *Talanta*, 178 (2018) 449.
41. G.L. Zhang, H.P. Fu, D. S. Zou, R. L. Xiao, J. Liu, S. J. Li, *Int. J. Electrochem. Sc.*, 12 (2017) 11465.

© 2019 The Authors. Published by ESG (www.electrochemsci.org). This article is an open access article distributed under the terms and conditions of the Creative Commons Attribution license (<http://creativecommons.org/licenses/by/4.0/>).